The pH-Dependent Stability of Wild-type and Mutant Transthyretin Oligomers

S. Skoulakis and J. M. Goodfellow
Department of Crystallography, Birkbeck College, University of London, London WC1E 7HX, UK

ABSTRACT A reduction in pH is known to induce the disassociation of the tetrameric form of transthyretin and favor the formation of amyloid fibers. Using continuum electrostatic techniques, we calculate the titration curves and the stability of dimer and tetramer formation of transthyretin as a function of pH. We find that the tetramer and the dimer become less stable than the monomer as the pH is lowered. The free energy difference is 13.8 kcal/mol for dimer formation and 27 kcal/mol for tetramer formation, from the monomers, when the pH is lowered from 7 to 3.9. Similar behavior is observed for both the wild-type and the mutant protein. Certain residues (namely Glu-72, His-88, His-90, Glu-92, and Tyr-116), play an important role in the binding process, as seen by the considerable $pK_{1/2}$ change of these residues upon dimer formation.

INTRODUCTION

Amyloidosis is a process in which a soluble protein aggregates irreversibly into insoluble fibrils. Apparently unrelated proteins can form these amyloids fibers, which are associated with a number of different diseases (Dobson, 1999). In vitro studies have shown that for a number of specific proteins, amyloids eventually form under partially denaturing conditions such as heat or addition of acid. It has become clear that a core β-sheet structure is formed in all amyloids leading to a common quaternary and tertiary structure (Kelly, 1997). Understanding of fibrillogenesis in detail at the molecular level is still lacking, but it has been proposed that the fibril formation may be a generic property of all proteins (Dobson, 1999). In vivo, the conditions inside the cell are controlled in a way to prevent the partial unfolding of proteins. When there is a loss of regulation, for example due to ageing or mutations, partial unfolding may occur that eventually leads to the formation of amyloids.

Transthyretin (TTR), formerly known as prealbumin (Blake et al., 1978), is one of at least 20 of human proteins that under suitable conditions has been shown to form amyloids (Kelly 1997; Damas and Saraiva, 2000). Deposits of wild-type TTR amyloids accumulate in the heart, in a disease called senile systemic amyloidosis (SSA) with the age of onset at about 80. A related disease, familial amyloidotic polyneuropathy (FAP), occurs at a much younger age, in some cases during the second decade of life, and affected individuals are found to have a mutation of TTR. So far 73 point mutations are associated with FAP and many of these destabilize the molecule leading to the formation of fibrils.

Many structures of TTR and of its mutants, amyloidogenic or nonamyloidogenic, have been determined (Hörnberg et al., 2000). The physiologically active form of wild-type TTR is a homotetrameric plasma protein the monomer of which is composed of 127 amino acid residues (Fig. 1). The residues in the monomeric unit are in two four-stranded β-sheets, which form a β-sandwich structure. In general, all mutant structures crystallize in the same space group as the wild-type, and display only minor changes compared with wild-type TTR. Nevertheless it has been shown the tetramer of the amyloidogenic mutants is less stable in vitro than the wild-type under acidic conditions (Nettleton et al., 1998).

One of the models that has been proposed for the formation of amyloids is the conformational change hypothesis (Kelly, 1998). First, by lowering the pH the tetrameric structure of the protein is disrupted and is disassociated into a monomeric structure, which is structurally different from the monomer at normal pH (Fig. 2). These altered monomers can associate and eventually form amyloid fibers. The mutations shift the tetramer-monomer equilibrium in favor of the structurally altered monomer, leading to a relative loss of stability of the mutated proteins relative to the wild-type.

The pH-dependent effects in proteins are mainly electrostatic in nature and originate from changes in the protonation states of acidic and basic residues (Yang and Honig, 1993; Schaefer et al., 1997; Ullmann and Knapp, 1999). Some of the titratable residues in a protein exhibit different behavior, compared with that of the isolated residues, due to their interactions with other residues in the protein, and the altered interactions with the solvent. The classical continuum treatment of the electrostatic interactions of a protein in aqueous solvent is obtained by solving the Poisson-Boltzmann equation (Warwicker and Watson, 1982; Gilson and Honig, 1988; Honig and Nicholls, 1995) as follows:

$$\nabla[\varepsilon(r)\nabla\phi(r)] - k^2\varepsilon(r)\ \sinh[\phi(r)] = -4\pi\rho(r), \quad (1)$$

where $\phi(r)$ is the electrostatic potential at position r, $\rho(r)$ is the charge density, $\varepsilon(r)$ is the dielectric constant as a function of position, and k^2 is the modified Debye-Huckel parameter, which accounts for counterion screening in the solvent. Since water is more easily polarized by an electric field than

Submitted March 14, 2002, and accepted for publication December 13, 2002.

Address reprint requests to Spiros Skoulakis, Dept. of Crystallography, Birkbeck College, University of London, Malet Street, London WC1E 7HX, UK. Tel.: 0044-020-76316800; Fax: 0044-020-76316803; E-mail: s.skoulakis@mail.cryst.bbk.ac.uk.

0006-3495/03/05/2795/10 $2.00

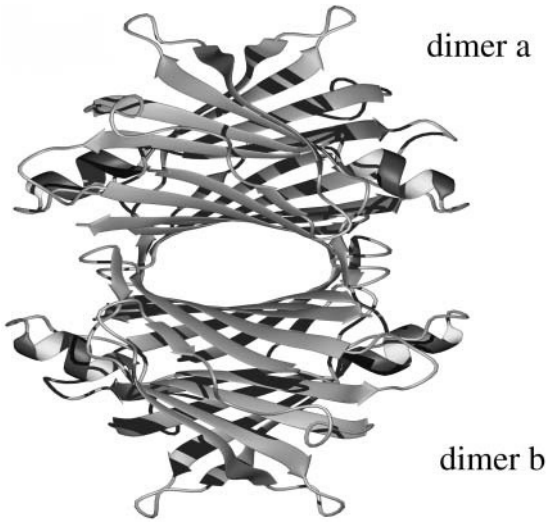

FIGURE 1 Diagram of the tetramer of wild-type transthyretin taken from crystal structure wt2, plotted using Molmol (Koradi et al., 1996) (version 2.1k.1.0).

the protein, at least two values for ε must be used. The Poisson-Boltzmann equation can be solved analytically only for simple cases. So numerical methods have to be used for its solution in realistic protein models. Warwicker and Watson (1982), were the first to publish a numerical solution based on a finite-difference scheme. Since then these methods have been developed and new boundary-element (Zauhar and Varnek, 1996) and multigrid (Holst and Saied, 1995) approaches have been applied. The calculation of electrostatic interactions by the Poisson-Boltzmann equation has been applied to studies of enzymatic mechanisms, proton transfer across membranes, redox reactions, and protein-protein association, (see Ullmann and Knapp, 1999 for an review).

In this paper, we study the stability of the tetramer and dimer relative to the monomer of wild-type TTR and two of its mutants as the pH is lowered. We have chosen two mutants, one which is amyloidogenic (V30M) and one which is nonamyloidogenic (T119M).

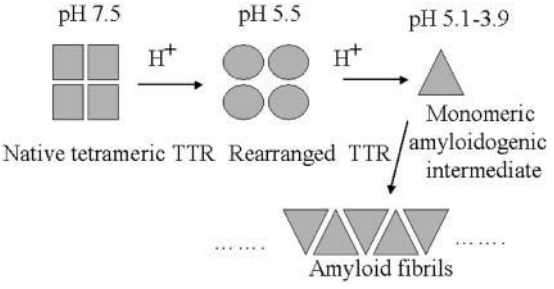

FIGURE 2 Diagram depicting the conformational change hypothesis for the formation of amyloid fibrils, from Kelly (1998). When the pH is decreased the pH the tetrameric structure disassociates into an altered monomeric structure, which eventually leads to amyloid fibrils.

METHODS

Model building

Initial models are constructed using the GROMACS package (Berendsen et al., 1995). The atomic coordinates are taken from the RCSB Protein Data Bank for the wild-type transthyretin (1tta) and (1f41) at 1.7-Å and 1.5-Å resolution, respectively, and the mutants M119T (1bze) at 1.8-Å and V30M (1ttc) at 1.7-Å resolution. Only the coordinate files of the dimers are provided and the tetramers are generated using the CCP4 suite of programs. As explained in Hörnberg et al. (2000), the placement of the first nine and the last two residues is not correct in the above pdb files due to the increased flexibility of these segments. We exclude these segments from all the structures in our pK_a calculations and since these are exposed to the solvent, we do not expect their pK_a values to be significantly perturbed. The positions of hydrogen atoms, that are added to the structures, are minimized using 50 cycles of steepest descent followed by conjugate gradient with a force tolerance of 100 kJ/mol/nm. During this minimization procedure, all the atoms except those of hydrogen are frozen.

Electrostatic calculations and titration curves

The electrostatic potential can be found by solving the linearized form of Poisson-Boltzmann equation:

$$\nabla[\varepsilon(r)\nabla\phi(r)] - k^2\varepsilon(r)\phi(r) = -4\pi\rho(r), \tag{2}$$

where the variables are the same as in Eq. 1. If there are changes in the titration of the residues upon binding of the monomer to form the dimer (or dimer to form tetramer), then the stability will be pH dependent. This is compactly expressed by the equation:

$$\partial\Delta G/\partial\mathrm{pH} = 2.303RT[\langle Q\rangle_{\mathrm{fin}} - \langle Q\rangle_{\mathrm{in}}], \tag{3}$$

where ΔG is the free energy difference for the process with final state (fin) with mean charge $\langle Q\rangle_{\mathrm{fin}}$ and initial state (in) with mean charge $\langle Q\rangle_{\mathrm{in}}$. The mean charge for a conformation (a), $\langle Q\rangle_{\mathrm{a}}$, may be calculated for each pH step if we know the titration behavior of the residues from the following formulae

$$\langle Q\rangle_{\mathrm{a}} = \sum_{\mathrm{i}=1}^{\mathrm{N}}\langle q(i)\rangle_{\mathrm{a}}, \tag{4}$$

$$\langle q(i)\rangle_{\mathrm{a}} = \sum_{\mathrm{s}}\delta_{\mathrm{n}}(i)\gamma_{\mathrm{n}}(i)\ \exp[-\Delta G_{\mathrm{a}}/RT]/\sum_{\mathrm{s}}\ \exp[-\Delta G_{\mathrm{a}}/RT], \tag{5}$$

$$\Delta G_{\mathrm{a}} = \sum_{\mathrm{k}=1}^{\mathrm{N}}[\delta_{\mathrm{n}}(k)\gamma_{\mathrm{n}}(k)2.303RT(\mathrm{pH} - \mathrm{pK}_{\mathrm{k}}^{\mathrm{int}}) + \sum_{1\le \mathrm{j}<\mathrm{k}}^{\mathrm{N}}\delta_{\mathrm{n}}(k)\delta_{\mathrm{n}}(j)\Delta G_{\mathrm{kj}}], \tag{6}$$

where $\langle q(i)\rangle_{\mathrm{a}}$ is the mean charge of the titratable residue (i), in a protein with conformation (a), with a total of N titratable residues, $\delta_{\mathrm{n}}(k)$ is 1 when the residue k is charged and 0 when it is neutral, $\gamma_{\mathrm{n}}(k) = -1$, 1 for an acidic and a basic group, respectively, s is the set of charge states in the protein and takes values n from 1 to 2^{N}, and R is the gas constant. ΔG_{kj} is the energy of interaction between residues k and j. It is calculated from the formula

$$\Delta G_{\mathrm{kj}} = \Delta G_{\mathrm{kj}}(1,1) - \Delta G_{\mathrm{kj}}(1,0) - \Delta G_{\mathrm{kj}}(0,1) + \Delta G_{\mathrm{kj}}(0,0), \tag{7}$$

where $\Delta G_{\mathrm{kj}}(\delta_{\mathrm{n}}(k), \delta_{\mathrm{n}}(j))$ is the interaction free energy in kcal/mol between amino acids k and j in their charge states defined by $\delta_{\mathrm{n}}(k)$ and $\delta_{\mathrm{n}}(j)$. Also the intrinsic pK_a (pK^{int}) of an ionizable group is defined as the pK_a it would have if all the other ionizable residues were neutral, and is given by

$$pK_k^{int} = pK_k^0 - \gamma(k)\Delta\Delta G_k/2.303RT, \quad (8)$$

where pK_i^0 is the pK_a of an isolated residue (i) in solution. $\Delta\Delta G_i$ is the change in the electrostatic energy, as calculated from Poisson-Boltzmann equation, of charging a titratable group (i) in a neutral protein relative to charging it isolated in a model compound in solution.

$$\Delta\Delta G_k = \Delta G_k^{protein} - \Delta G_k^{model}. \quad (9)$$

We can define the pK_a values on the basis of protonation probability $\langle q \rangle$ from the equation:

$$pK_a = pH + (1/2.303)\ \ln[\langle q \rangle/(1 - \langle q \rangle)]. \quad (10)$$

The pH value at which the protonation probability is 0.5 is called $pK_{1/2}$ and is often used to describe the titration behavior of the residues. If there is an isolated titratable residue, with no interactions with other residues the titration curve would follow the Henderson-Hasselbalch equation,

$$\langle q(i) \rangle = \exp 2.303(pK_i^{int} - pH)/(1 + \exp 2.303(pK_i^{int} - pH)), \quad (11)$$

but the interactions between the residues complicate the expression.

The calculations are performed using version 1.1.8 of the MEAD (Macroscopic Electrostatics with Atomic Detail) program (Bashford and Gerwert, 1992). We use two force fields, namely the PARSE (Sitkoff et al., 1994) and the Gromos96 force field (van Gunsteren et al., 1996), in the calculations but with modified charges. Following previous work (Demchuk and Wade, 1996), we do not include extra hydrogen atoms when these are not present in the form of the titratable residues at normal values of pH, but we modified the Gromos96 force field as described in Table 1. We have also used different values for the charges from the ones shown in Table 1, with no noticeable change in the pK_a values. We have calculated the pK_a values with the relative dielectric constant set at both 20 and 80. For the monomers a two-step focusing method is employed using an initial 81^3 grid with 1-Å spacing centered on the geometric center of the protein, followed by a 81^3 grid with 0.25-Å spacing centered at the titrating residues. For the tetramers and dimers, the same procedure is followed but the grid used is 121^3. Therefore we have also tried to include the conformational flexibility explicitly by performing short (100 ps) molecular dynamics simulations with explicit solvent, and then clustering the results to find the most populated conformations during the trajectory. The GROMACS package is used for the molecular dynamics calculations. We find that the pK_a values do not change by more than 1 pK_a unit. In principle, from Eqs. 4, 5, and 6 we can calculate the mean protonation state of every residue. Since the statistical average involves 2^N states for N ionizable residues, it is impractical for our case with several tens of ionizable groups. Therefore we use a Monte-Carlo technique as implemented in the program Monti (Beroza et al., 1990). At each step of 0.1 pH units, 1000 full steps of Monte Carlo are performed followed by 5000 reduced steps in which the residues most likely to be protonated or deprotonated are omitted from the sampling.

TABLE 1 Partial electronic charges for titrating residues

			Fractional electronic charge state*	
Residue	pK^0	Atom	$s = 0$	$s = 1$
Arg	12.0	CD	0.090	0.000
		NE	−0.110	−0.150
		HE	0.240	0.150
		CZ	0.340	0.200
		NH1	−0.260	−0.400
		HH11	0.240	0.150
		HH12	0.240	0.150
		NH2	−0.260	−0.400
		HH21	0.240	0.150
		HH22	0.240	0.150
Lys	10.4	CD	0.000	0.000
		CE	0.127	0.000
		NZ	0.129	−0.840
		HZ1	0.248	0.280
		HZ2	0.248	0.280
		HZ3	0.248	0.280
Tyr	9.6	CZ	0.150	−0.200
		OH	−0.548	−0.800
		HH	0.398	0.000
Cys	8.4	SG	−0.064	−1.064
		HG	0.064	0.064
His(A)	6.4	CB	0.000	0.000
		CG	−0.050	0.000
		ND1	0.380	0.000
		HD1	0.300	0.190
		CD2	0.000	0.130
		CE1	−0.240	0.260
		NE2	0.310	−0.580
		HE2	0.300	0.000
His(B)	6.8	CB	0.000	0.000
		CG	−0.050	0.130
		ND1	0.380	−0.580
		HD1	0.300	0.000
		CD2	0.000	0.000
		CE1	−0.240	0.260
		NE2	0.310	0.000
		HE2	0.300	0.190
Glu	4.4	CD	0.270	0.270
		OE1	−0.135	−0.635
		OE2	−0.135	−0.635
Asp	4.0	CG	0.270	0.270
		OD1	−0.135	−0.635
		OD2	−0.135	−0.635

Charges compatible with the Gromos96 forcefield.
*The charge sets are $s = 0$ for the unprotonated and $s = 1$ for the protonateted states. His(A), His(B) are the two possible states for a charged histidine.

Stability analysis

The free energy of binding of an assembly of n monomers is given by

$$\Delta G_{bind} = G_{oli} - n \times G_{mon}, \quad (12)$$

where G_{oli} and G_{mon} are the free energies for the oligomers and the monomer structures, respectively. By integrating Eq. 2, (Yang and Honig, 1993), we can determine an expression for the electrostatic free energy of binding ($\Delta\Delta G_{bind}$ (pH, pH_0)), relative to a value $\Delta G_{bind}(pH_0)$ at a reference pH_0:

$$\Delta\Delta G_{bind}(pH, pH_0) = \Delta G_{bind}(pH) - \Delta G_{bind}(pH_0) = 2.303RT \int_{pH_0}^{pH} \Delta\langle Q(pH')\rangle\, dpH', \quad (13)$$

where, $\Delta\langle Q(pH)\rangle$ is the pH-dependent mean charge difference between two states of the system and is given by a similar equation to Eq. 12

$$\Delta\langle Q\rangle_{bind} = \langle Q\rangle_{oli} - n \times \langle Q\rangle_{mon}, \quad (14)$$

where $\langle Q\rangle_{oli}$ and $\langle Q\rangle_{mon}$ are the mean charges for the oligomer and monomer respectively. The reference value pH_0 is arbitrary and the $pH_0 = 0$ has appeared in the literature. Schaefer et al. (1997) has shown that by taking $pH_0 = \infty$, we can calculate relative and absolute changes in the free

TABLE 2 $pK_{1/2}$ values for TTR monomers

	mut_noa		wt1		wt2		mut_a	
Residues	$\varepsilon = 20$	$\varepsilon = 80$	$\varepsilon = 20$	$\varepsilon = 80$	$\varepsilon = 20$	$\varepsilon = 80$	$\varepsilon = 20$	$\varepsilon = 80$
Arg-21	11.1	12.0	11.6	12.1	11.4	12.0	11.4	12.0
Arg-34	11.4	12.0	11.6	12.1	11.4	12.0	11.7	12.0
Arg-103	12.0	12.0	11.9	12.1	12.0	12.0	12.0	12.0
Arg-104	11.4	11.7	11.6	11.8	11.4	11.7	11.4	11.7
Lys-15	9.6	10.2	9.5	10.0	9.5	9.9	9.6	10.2
Lys-35	9.6	9.9	9.8	10.0	9.8	9.9	9.3	9.9
Lys-48	10.2	10.2	10.1	10.0	9.3	10.2	9.9	10.2
Lys-70	9.3	9.9	9.2	10.0	9.3	9.9	9.3	9.9
Lys-76	9.9	10.2	9.8	10.0	9.6	10.2	9.6	9.9
Lys-80	10.2	10.2	10.1	10.0	9.9	9.9	9.9	9.9
Tyr-69	9.3	8.4	10.4	8.5	9.9	8.7	10.2	8.7
Tyr-78	8.7	8.4	9.2	8.2	8.7	8.7	9.3	8.4
Tyr-105	9.3	8.7	9.2	8.5	8.7	8.7	9.3	8.7
Tyr-114	9.6	9.3	9.5	9.1	9.6	9.0	9.6	9.3
Tyr-116	9.3	8.7	9.2	8.8	9.6	8.7	9.3	8.7
Cys-10	8.1	7.2	7.7	7.3	7.5	7.2	7.8	7.2
His-31	5.1	5.4	5.0	5.5	5.1	5.4	5.1	5.4
His-56	4.8	5.4	4.1	5.5	4.8	5.1	5.1	5.4
His-88	3.9	5.1	4.1	5.2	3.9	5.1	3.9	5.1
His-90*	3.6	4.8	4.1	4.9	3.8	4.8	3.9(A)	4.8
Glu-42	2.4	2.4	3.2	2.8	3.0	2.7	2.7	2.4
Glu-51	3.6	3.6	3.5	3.1	3.6	3.6	3.6	3.3
Glu-54	2.1	2.1	1.7	1.9	1.8	1.8	1.8	2.1
Glu-61	3.3	2.7	2.9	2.5	3.0	2.7	3.3	3.3
Glu-62	3.3	3.6	3.5	3.4	3.3	3.6	3.6	3.6
Glu-63	3.3	3.0	2.9	2.8	3.0	2.7	3.0	2.7
Glu-66	3.6	3.3	3.8	3.4	3.6	3.3	3.9	3.3
Glu-72	0.9	1.2	0.5	1.0	1.2	0.9	0.6	0.9
Glu-89	2.1	2.1	2.0	2.2	2.1	2.1	2.1	2.1
Glu-92	0.3	0.9	0.5	1.0	0.3	1.2	0.3	0.9
Asp-18	−0.8	0.9	−0.1	1.3	−0.8	1.2	−0.4	1.2
Asp-38	3.0	2.7	2.6	2.8	2.7	2.7	2.7	2.7
Asp-39	2.4	2.1	2.6	2.2	2.4	2.4	2.4	2.1
Asp-74	0.9	0.9	0.2	0.7	0.3	0.9	0.9	0.9
Asp-99	1.8	1.8	2.0	2.2	2.1	1.8	1.8	2.1

$pK_{1/2}$ is defined as the pK_a value at which the probability is 0.5, Eq. 10. Comparison of the $pK_{1/2}$ values for wild-type wt1 (tta), wt2 (f41) and the V30M mutant mut_a (ttc), and M199T mut_noa (bze) one. We use two dielectric constants $\varepsilon = 20$ and $\varepsilon = 80$.

*Two calculations are performed for the histidines with His(A) and His(B). When His(A) is found more preferable, the results are indicated with (A). Most of the values are reasonable. The low values for Glu-72, Glu-92, Asp-18, and Asp-74 can be explained by the proximity of other residues as explained in the text.

energy as a function of pH. We will use this reference pH scale to calculate the relative energy changes from the equation

$$\Delta\Delta G_{\text{bind}}(\text{pH}) = -2.303RT \int_{\text{pH}}^{\infty} \Delta\langle Q(\text{pH}')\rangle d\text{pH}'. \qquad (15)$$

This equation is used to calculate the stability of the dimer relative to the monomer and the tetramer relative to the dimer.

RESULTS

Initially we undertook calculations to determine the titration curves of all the residues in the monomer, dimer and tetramer of wild-type and mutant conformations. Using MEAD we solve the Poisson-Boltzmann equation and we calculate the pK^{int} values as described above in Eqs. 4–8. We use dielectric constant ε, 20 and 80. These pK^{int} values, and the matrix of interactions are used as input for Monti to calculate the titration behavior of the residues. The titration curves of the residues in the wild-type are similar to those of the mutants, which is consistent with the close structural similarity of the wild-type and mutant conformations.

The results of the $pK_{1/2}$ calculations for the monomers of the nonamyloidogenic mutant M119T (mut_noa), the amyloidogenic mutant V30M (mut_a), and the two structures for the wild-type 1tta (wt1), f41 (wt2), are shown in Table 2. For most of the residues, the titration curve follows the sigmoidal form of the Henderson-Hasselbalch equation. In these cases, we can use the $pK_{1/2}$ values of the titration curves to compare with the pK^{int} values (Table 3). Only residue His-90 is calculated to have a different form of titration curve (Fig. 3).

TABLE 3 pK^{int} for the TTR monomers

	mut_noa		wt1		wt2		mut_a	
Residue	$\varepsilon = 20$	$\varepsilon = 80$	$\varepsilon = 20$	$\varepsilon = 80$	$\varepsilon = 20$	$\varepsilon = 80$	$\varepsilon = 20$	$\varepsilon = 80$
Arg-21	11.5	12.0	11.6	12.0	11.8	12.0	11.7	12.1
Arg-34	11.7	12.1	11.8	12.1	11.9	12.1	11.9	12.2
Arg-103	12.3	12.1	12.1	12.2	12.0	12.1	12.1	12.2
Arg-104	11.8	12.0	11.7	12.0	11.8	12.0	11.7	12.0
Lys-15	9.9	10.4	9.9	10.4	9.9	10.4	10.0	10.4
Lys-35	10.2	10.4	10.2	10.4	10.2	10.4	10.0	10.4
Lys-48	10.4	10.5	9.9	10.4	10.4	10.4	10.4	10.4
Lys-70	10.0	10.4	10.0	10.4	9.9	10.3	10.0	10.4
Lys-76	10.3	10.5	10.3	10.5	10.4	10.5	10.3	10.5
Lys-80	10.5	10.5	10.4	10.5	10.5	10.5	10.3	10.5
Tyr-69	10.9	9.6	11.2	9.7	11.5	9.7	11.4	9.7
Tyr-78	10.6	9.5	10.6	9.6	10.5	9.6	11.0	9.7
Tyr-105	10.4	9.6	10.0	9.5	10.4	9.5	10.4	9.6
Tyr-114	9.8	9.6	9.9	9.6	9.8	9.6	9.9	9.6
Tyr-116	9.9	9.5	10.0	9.5	9.8	9.5	9.8	9.5
Cys-10	9.1	8.2	8.3	8.2	8.8	8.2	8.4	8.2
His-31	6.4	6.7	6.4	6.8	6.4	6.7	6.4	6.7
His-56	6.2	6.6	6.3	6.6	6.0	6.6	6.4	6.7
His-88	5.8	6.7	5.8	6.7	5.7	6.6	5.8	6.7
His-90	6.0	6.6	6.1	6.7	6.0	6.6	6.2	6.7
Glu-42	4.9	4.4	4.9	4.5	4.8	4.5	5.0	4.4
Glu-51	4.5	4.3	4.6	4.3	4.4	4.4	4.7	4.4
Glu-54	4.5	4.2	4.5	4.2	4.3	4.1	4.4	4.2
Glu-61	5.2	4.5	4.9	4.4	4.8	4.4	4.6	4.4
Glu-62	4.5	4.4	4.4	4.4	4.3	4.3	4.3	4.4
Glu-63	4.8	4.4	4.6	4.4	4.8	4.4	4.9	4.4
Glu-66	4.8	4.5	4.8	4.6	4.7	4.5	4.8	4.6
Glu-72	4.9	4.4	5.0	4.4	4.8	4.3	5.0	4.4
Glu-89	4.7	4.4	4.8	4.4	4.9	4.4	4.8	4.4
Glu-92	5.0	4.4	5.0	4.4	4.4	4.2	5.6	4.4
Asp-18	4.0	3.7	4.0	3.7	4.2	3.7	4.2	3.7
Asp-38	3.8	3.8	3.8	3.7	3.8	3.8	3.8	3.8
Asp-39	4.3	4.0	4.3	4.0	4.3	4.1	4.3	4.0
Asp-74	4.0	3.8	4.4	3.9	4.1	3.8	4.1	3.8
Asp-99	4.2	4.0	4.3	4.0	4.3	4.0	4.3	4.0

pK^{int} values are calculated from Eq. 8. The lower values of Table 2 for the pK_a values, indicate the importance of the interactions between titratable residues. These interactions are not included in the calculation of pK^{int}. The calculations are performed with dielectric constant 20 and 80.

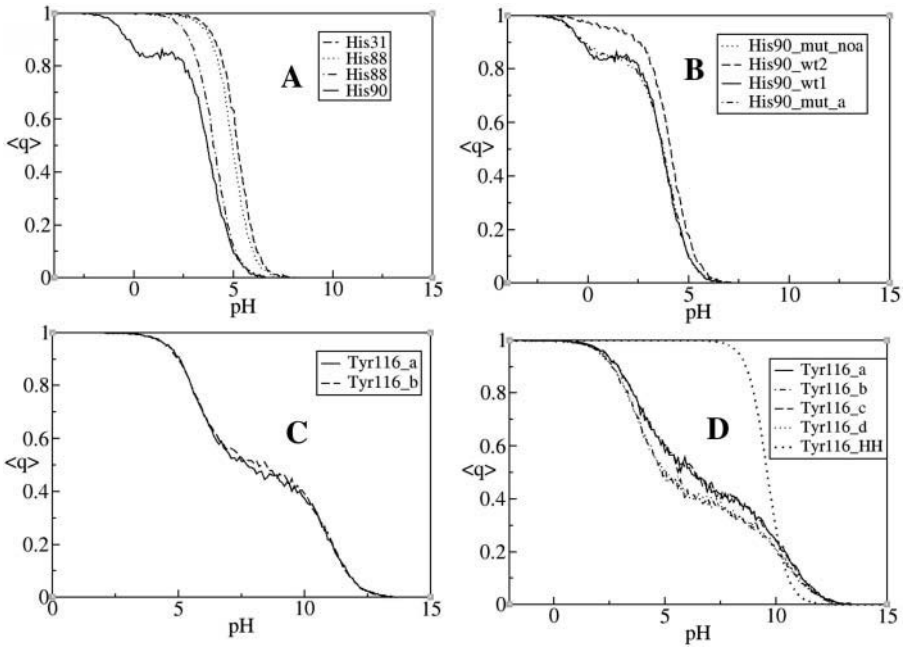

FIGURE 3 Mean titration curves $\langle q \rangle$, calculated with $\varepsilon = 20$ (*a*) for histidine residues in a monomer from the crystal structure wt1, (*b*) for residue His90 in all monomers from crystal structures, (*c*) for the residue Tyr-116 in the two monomer a (Tyr-116_a) and b (Tyr-116_b), of the dimer, and (*d*) for residue Tyr-116 in the tetramer. The Henderson-Hasselbalch titration curve (Tyr-116_HH) with the same $pK_{1/2}$ value is also shown.

The mean value of the charge $\langle q \rangle$ is calculated from Eqs. 4, 5, and 6 and is shown in Fig. 3 for His-90 and for the other His residues which behave normally. The form of these curves is very similar for wt1, and the mutants, but the anomalous behavior is not as profound in the wt2. The mean total charge, $\langle Q \rangle$, behaves similarly with the change of pH (Fig. 4) for all the structures, with maximum difference 0.3 in the pH range 7–3.9.

For all residues, the $pK_{1/2}$ value is reduced with respect to the pK^{int} and pK^{0} values. The pK^{int} values account for the interaction of the residues with the background charges and for the dissolvation effect. As the $pK_{1/2}$ values are lower than pK^{int}, there must be further interactions to account for the discrepancy and these interactions are due to the strongly interacting titratable residues.

Most of the residues have reasonable $pK_{1/2}$ values. His-88, His-90, Glu-42, Glu-54, Glu-72, Glu-92, Asp-18, Asp-74, and Asp-99 have lower values than expected. Due to the long range of the electrostatic interactions and the number of residues, it is not easy, in general, to attribute the anomalous $pK_{1/2}$ value to the proximity of specific residues. However, the interactions between the residues can be analyzed from visual inspection of the crystal structures and from the matrix of interactions (as output from MEAD). We find that there is a network of strongly interacting residues, consisting of Glu-72, His-88, Glu-92, His-90, and Tyr-116. The distances between the closest atoms are shown in Table 4. These are the residues that are found to be strongly interacting from the matrix of interactions. We also find that Glu-42 is influenced by Arg-34, Glu-54 by Lys-15, Asp-18 by Tyr-78, and Asp-99 by Tyr1-05.

Upon dimer formation, the pK_a of some the residues changes and the results for only the largest changes are shown in the Table 5. These changes cannot easily be explained by the approach of the other monomer or for example by formation of salt bridges. The only extra hydrogen bond that is formed involving titratable residues is between OG1 (Thr-96) and OE2 (Glu-89). Notable is the close proximity of Glu-92 in one monomer to the Glu-92 and the OH atom of Tyr-116 in the other monomer. These belong to the network of strongly intramolecularly interacting residues, that become buried upon dimer formation (Table 6, Table 7, and Fig. 5), and interact intermolecularly with the same network of the other monomer. We have found, from the matrix of interactions, that the intramonomer interactions themselves are changed by the presence of the second monomer, because the residues in the interface become buried and also because the strength of the interactions between the titratable residues change inside the dimer. The importance of the interactions between the titratable residues is again very significant as the pK^{int} changes are less than the corresponding $pK_{1/2}$ ones, or even in some cases have a different sign.

His-90 once more has a nonstandard titration curve in both monomers, but now has a much lower $pK_{1/2}$ value. Tyr-116 appears to have a different titration curve, with respect to the monomer, and this is explained by the proximity of Glu-92 and Tyr-116 from the second monomer upon dimer formation, (Table 7 and Fig. 5).

The mean protonation charge, $\langle Q \rangle$, for the dimers, is similar for all structures with maximum difference 0.6 in the pH range 7–3.9 (Fig. 4). This change in $\langle Q \rangle$upon dimer formation leads to the different stability of the dimer relative to the monomer, as we lower the pH (Fig. 6). We observe that this curve has a local minimum at pH 8.5. This is ex-

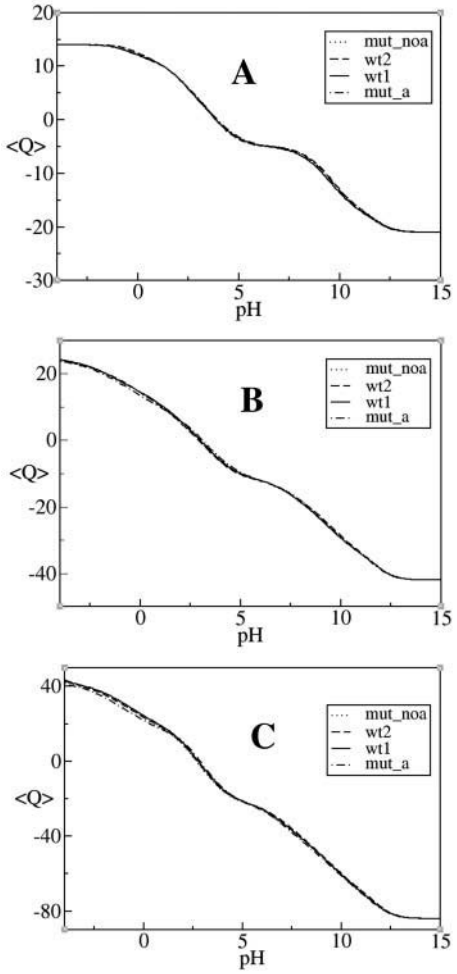

FIGURE 4 The mean total titration curve $\langle Q \rangle$, with $\varepsilon = 20$, as a function of pH, as calculated from Eq. 4, for (*a*) the monomer, (*b*) dimer, and (*c*) tetramer, respectively.

plained by the change in the protonation curves of the basic residues, lysines and tyrosines. The acidic residues, mainly the histidines, make an important contribution below pH 5. Similar curves occur for all the structures we use.

The relative free energy difference upon dimer formation ($\Delta\Delta G$) is calculated by integrating the above curve according to Eq. 15 (Fig. 7). It is apparent that the dimer becomes less stable with respect to the monomer as the pH decreases. This change is more rapid below pH $\approx$ 3.5 and all structures studied so far behave similarly. The contribution of individual residues to the stability can be calculated from Eq. 15. It follows that sites with $\Delta\langle Q \rangle < 0$ increase the free energy of the oligomer. They are destabilizing as they lead to a loss of stability upon variation of pH.

For the wild-type wt1, there is a difference of 13.8 kcal/mol when the pH is lowered from 7 to 3.9. We use these values to compare our results with the conformational change hypothesis. Similar behavior is exhibited by the other structures, with energies 13.7, 14.2, and 14.6 for wt2, mut_a, and mut_noa, respectively. Thus to discriminate the mutants from the wild-type is difficult with this type of analysis. The free energy difference between the two wild-type structures is 0.1 kcal/mol for pH values between 7 and 3.9. We find this estimate from the mean value, within the pH range 7–3.9, of the difference, in the free energy change upon dimer formation, between the two structures of the wild-type. The mutants differ from the wild-type by 0.5–0.6 kcal/mol and are predicted to be more stable than the wild-type, in contrast to the experimental results. The energy difference we find between wild-type and mutants is only 0.5–0.6 kcal/mol, making any discrimination unreliable. The difference in energy between the two wild-type structures is found to be due to the tyrosine residues, mainly Tyr114, Tyr105, and Tyr78. This causes the free energy curves of the structures

TABLE 4 Close contacts within the monomers

	Distances (Å)			
Closest nonhydrogen atoms	mut_noa	wt1	wt2	mut_a
Glu-72(OE1)-His-90(NE2)	4.12	3.84	4.55	4.29
His-90(NE2)-Glu-92(OE2)	5.90	4.26	5.61	4.26
His-90(ND1)-Glu-92(OE1)	5.60	4.57	3.29	4.65
His-90(ND1)-Glu-92(OE2)	4.19	2.57	5.83	3.39
Glu-92(OE1)-Tyr116(OH)	3.44	3.74	5.27	7.60
His-88(NE2)-Tyr-116(CE2)	3.84	3.70	6.17	3.90
His-88(NE2)-Tyr-116(OH)	5.20	4.95	3.99	5.29
His-88(ND1)-Tyr-116(CE2)	3.81	3.92	5.29	3.93

TABLE 5 $\Delta pK_{1/2}$ for dimer formation, monomer a

	mut_noa		wt1		wt2		mut_a	
	$\varepsilon = 20$	$\varepsilon = 80$	$\varepsilon = 20$	$\varepsilon = 80$	$\varepsilon = 20$	$\varepsilon = 80$	$\varepsilon = 20$	$\varepsilon = 80$
Lys-35	−0.8	−0.3	−1.0	−0.6	−0.8	−0.3	−0.9	−0.5
Lys-70	−1.9	−0.7	−2.1	−1.0	−2.4	−0.9	−2.5	−0.7
Lys-76	−1.1	−0.6	−1.2	−0.6	−1.0	−0.8	−1.6	−0.5
Tyr-105	−1.1	−0.7	−1.3	−0.7	−1.6	−1.1	−1.1	−0.7
Tyr-114	−1.0	−0.7	−1.2	−0.5	−1.1	−0.4	−1.2	−0.6
Tyr-116	−1.7	−1.5	−1.6	−1.4	0.0	−1.3	−1.5	−1.3
His-31	−0.9	−0.6	−0.9	−0.7	−0.8	−0.6	−0.7	−0.4
His-88	−5.3	−1.5	−5.3	−1.4	−5.7	−1.5	−5.7	−1.5
His-90	−7.6	−1.8	−7.4	−1.9	−6.9	−1.8	<−7.6*	−2.2
Glu-66	−0.4	−0.5	−0.4	−0.6	−0.6	−0.5	−0.7	−0.5
Glu-72	−2.3	−2.2	−2.8	−2.0	−2.7	−1.9	−2.6	−2.1
Glu-89	−2.5	−2.3	−2.5	−2.4	−2.8	−2.5	−3.9	−2.9
Glu-92	<−5.3*	−3.9	<−5.3*	−3.8	<−4.5*	−4.4	<−4.3*	−4.1
Asp-18	−0.8	−0.5	−0.4	−0.7	−0.5	−0.4	−0.6	−0.6
Asp-39	−1.8	−1.3	−2.0	−1.6	−1.4	−1.2	−2.0	−1.5
Asp-74	−0.9	−0.9	−0.7	−1.1	−0.6	−1.1	−0.9	−1.1
Asp-99	−2.4	−1.4	−2.1	−1.6	−2.2	−1.4	−1.8	−1.5

$\Delta pK_{1/2}$ values ($(pK_{1/2}$(dimer) − $pK_{1/2}$(monomer)) for the residues with the largest changes in values i.e., $|\Delta pK_{1/2}| > 0.6 \cong 0.8$ kcal/mol at 300 K. The values for the residues of only one monomer (a) are shown. Due to symmetry, we expect similar behavior for the other monomer (b). The values are calculated with dielectric constant ε, 20 and 80. His-90 and Tyr-116 have anomalous titration curves as shown in Fig. 3 and the $pK_{1/2}$ values for these residues is not very informative for the behavior of their titration curves.

*These residues titrate at a pH < –4 in the dimer.

TABLE 6 Accessible surface area for all structures

	ASA(dimer) Å^2				ASA(monomer) Å^2				Δ(ASA) Å^2			
Residues	wt1	wt2	mut_a	mut_noa	wt1	wt2	mut_a	mut_noa	wt1	wt2	mut_a	mut_noa
His-88	6.4	6.4	7.4	6.7	50.0	49.9	49.9	50.6	−43.6	−43.5	−42.5	−43.9
Glu-89	32.1	28.1	32.0	24.9	107.4	104.5	107.6	100.6	−75.3	−76.4	−75.6	−75.7
His-90	41.9	35.1	38.7	45.4	62.7	59.1	66.9	67.3	−20.8	−24.0	−28.2	−21.9
Glu-92	3.2	8.6	6.8	8.0	73.8	81.6	64.1	76.1	−70.6	−73.0	−57.3	68.1
Tyr-116	6.6	6.0	8.7	6.3	67.5	73.5	75.1	65.4	−60.9	−67.5	−66.4	−59.1

Upon dimer formation the above titratable groups become buried as shown from the change in the accessible surface area Δ(ASA) = (ASA(dimer) − (ASA(monomer)). All the numbers are in Å^2.

to slightly shifted with respect to each other. The most destabilizing residues in the pH range 3.5–7 are Tyr-116, His-88, and His-90 as they contribute the most at the total charge difference $\Delta\langle Q\rangle$, (Fig. 6) between oligomers.

On dimer association to form the tetramer, a similar pattern of behavior is observed. The values of $pK_{1/2}$, shown in Table 6, decrease but not to the same extent as upon the dimer formation. This is not surprising because the dimer-dimer interface is populated by hydrophobic residues. This is in contrast to the monomer-monomer interface which is occupied mainly by charged and polar residues. Once more the interactions between residues are the most important factor leading to the low $pK_{1/2}$ values. The most affected residues are the ones closest to the interface between the dimers, as expected, even though the only titratable residues that come closer than 5 Å to the dimer, due to tetramer formation, are Tyr-114 and Arg-21 from the third and fourth monomer of the second dimer. The appearance of the second dimer changes the strength of the interactions already present in the first dimer, and this causes the shift of the $pK_{1/2}$ values. The nonstandard titration curves for His-90 and Tyr-116 are still observed (as indicated in Fig. 3).

The free energy difference upon tetramer formation from the dimers, as we decrease the pH values from 7 to 3.9, is 8 kcal/mol for wt1 and 6.3, 10.9, and 9.8 for wt2, mut_a, and mut_noa, respectively (Fig. 7). The free energy difference between the two wild-type structures is 1.7 kcal/mol, making the two mutants indistinguishable and predicting both mutants to be more stable than the wild-type. The difference between wild-type and the mutants is mainly due to slight differences in the titration curves of Lys-15, Tyr-78 in all monomers. Even though we can predict the trend of the stability curve the calculations are not sensitive enough to discriminate the mutant from the wild-type structure, which is not surprising considering the high accuracy required for such discrimination. The contribution of all the residues in the binding interface is destabilizing. We would expect an increase of $\Delta\langle Q\rangle$ for some residues and thus a stabilizing role. Nevertheless the results once more indicate the importance of the network of electrostatic interactions of the charged residues and their importance in the pH related stability.

TABLE 7 New contacts upon dimer formation

		Distances (Å)			
Monomer a	Monomer b	mut_noa	wt1	wt2	mut_a
Glu-92(O)	Tyr-116(OH)	2.98	3.00	2.76	2.88
Glu-92(OE1)	Glu-92(OE1)	4.53	4.14	4.11	2.63
Glu-92(OE1)	Glu-92(OE2)	6.03	6.02	3.29	3.89
Glu-92(OE2)	Glu-92(OE1)	5.81	5.07	4.46	4.81
Tyr-116(OH)	Tyr-116(OH)	4.03	4.79	4.25	4.31

Upon dimer formation the above titratable groups come in close proximity resulting in low $pK_{1/2}$ values and anomalous titration curves.

DISCUSSION AND CONCLUSIONS

Even though the formulation of the problem is straightforward, there are uncertainties in the calculations of pK_a values in proteins (Bashford and Karplus, 1990, Antosiewicz et al., 1996, van Vlijmen et al., 1998b). These are due to the value of the dielectric constant, the force field used, and the use of one conformation in the calculations. Usually the force fields are the ones optimized for molecular dynamics calculations. It has been pointed out (Demchuk and Wade, 1996), that the placement of hydrogen atoms can cause problems in the pK_a calculations and has proposed an adjusted force field. The value of the dielectric constant is also a factor of concern. For the solvent a value of 80 is used, but for the protein, values from 2 up to 30 have been suggested. The large value is used to compensate for the omission of the conformational flexibility in the calculations (Simonson 2001; Sheinerman et al., 2000).

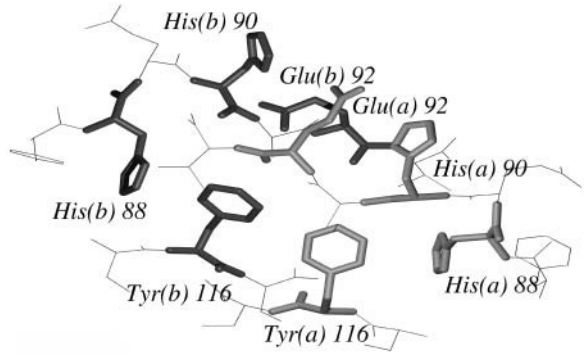

FIGURE 5 Geometry of important residues in monomer (*a*) and monomer (*b*), upon dimer formation of wt2. The distance between ND1 (His-90) and OE2 (Glu-92) is 2.90 Å, and between OE1 (Glu-92) OH (Tyr-116) is 3.12 Å.

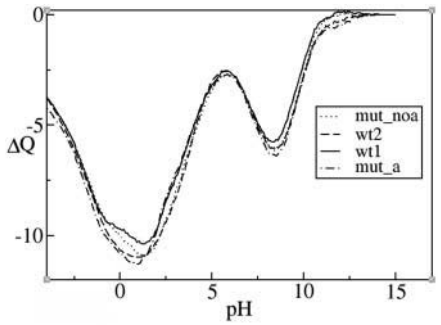

FIGURE 6 The change in total mean charge $\Delta Q = \langle Q \rangle_{dim} - \langle Q \rangle_{mon}$, with $\varepsilon = 20$, as a function of pH, for all crystal structures.

Conformational variability can have a substantial effect on the electrostatic interactions. Different methods have been used for explicitly including conformational flexibility in the electrostatic calculations (van Vlijmen et al., 1998) and references therein. Several conformations are generated using molecular dynamics and then averaged over the snapshots to get a representative conformation. After that we apply the methodology for finding the pK_a for this structure. Alternatively, the pK_a values are calculated for every structure of the trajectory and then the average titration curve is obtained. This approach is very demanding computationally. Moreover methods for coupling the averaging performed for finding the titration curve with average values for the electrostatic energies sampled over different side chain conformations have been used. We have performed short molecular dynamics calculations (100ps) simulations with explicit solvent, and then we have used clustering to find the most populated conformations during the trajectory.

Both charged and uncharged states have been used for histidines. We have then calculated the titration curves. The pK_a values, so calculated, do not change by more than 1 pK_a unit when the dielectric constant is $\varepsilon = 20$. Consequently there is no improvement in the stability curves. The short, 100ps, trajectories are not long enough to equilibrate the system and longer molecular dynamics simulations are needed to investigate the flexibility of the conformations. The use of lower values (namely 4 and 10) for the dielectric constant resulted in unrealistically low $pK_{1/2}$ values. By using $\varepsilon = 80$ we have found that the $pK_{1/2}$ values (Table 2) are more realistic with no anomalous titration curves appearing and the changes upon dimer, tetramer formation are in general slightly less than the results with dielectric constant of 20, (Tables 5 and 8). This can be thought as an indication that by lowering the pH there are substantial conformational changes, as Kelly proposes, that even a dielectric constant of 80 cannot compensate. A large value is used to account for the relaxation of the protein in the process that participates. Even if an extreme value of 80 is used we find substantial energy differences, indicating the importance of the electrostatic interactions and moreover the substantial conformational changes of the protein upon

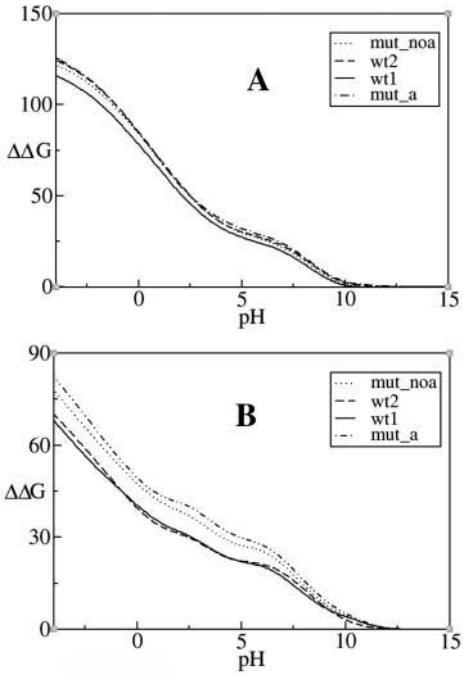

FIGURE 7 Free energy difference, $\Delta\Delta G$, in kcal/mol, with $\varepsilon = 20$ (*a*) upon dimer formation from the monomers and (*b*) tetramer formation from the dimers.

disassociation of the monomers. The short molecular dynamics simulations did not improve the pKa calculations, supporting the view of substantial conformational changes.

To get a more accurate result we would need the structure of the altered monomeric form at low pH values. In the experimental investigations of TTR stability it was shown that by lowering the pH only the monomer and not the dimer structure is populated. In our results we show the free energy differences upon dimer formation from the monomers and tetramer formation from the dimers. In order to make the results more comprehensible, the free energy difference for the tetramer formation from the monomers ($\Delta\Delta G$(tet-mon)), is calculated from adding the energies for dimer formation $\Delta\Delta G$(dim-mon) and tetramer formation from dimers ($\Delta\Delta G$(tet-dim)), according to the formula: $\Delta\Delta G$(tet-mon) = $\Delta\Delta G$(tet-dim) + $2\Delta\Delta G$(dim-mon). Using dielectric constant 20, we find that the free energy change for tetramer formation, from the monomers, is 27.4, 26.9, 31.1, and 32.2 in kcal/mol for wt1, wt2, mut_noa, and mut_a, respectively (Fig. 8). The statistical error is 0.5 kcal/mol making the discrimination between the structures unreliable. The error is calculated from the difference of the free energy between the two wild-type conformation we use. The overall trend of the stability curve is predicted but not relative stability between the structures. The above energy estimates maybe an overestimation since the conformational changes are not fully included in the calculations. Nevertheless they give an estimation of the energy change that is not available by other means. At present there are no equilibrium constant mea-

TABLE 8 $\Delta pK_{1/2}$ for tetramer formation, monomers a and b

	mut_noa		wt1		wt2		mut_a	
	$\varepsilon = 20$	$\varepsilon = 80$	$\varepsilon = 20$	$\varepsilon = 80$	$\varepsilon = 20$	$\varepsilon = 80$	$\varepsilon = 20$	$\varepsilon = 80$
Monomer a								
Lys-15	−2.5	−0.8	−2.1	−0.7	−1.8	−0.7	−2.3	−0.9
Tyr-78	−1.2	−1.1	−1.2	−0.9	−1.0	−1.0	−1.2	−1.0
Tyr-116	−2.4	−0.7	−1.7	−0.9	−2.9	−0.9	−3.0	−1.1
His-56	−0.8	−0.7	−1.0	−0.5	−1.1	−0.8	−1.0	−0.8
His-88	<−2.6	−1.6	<−2.6	−1.6	<−2.4	−1.5	<−2.2	−1.8
Glu-54	−2.6	−1.7	−2.5	−1.9	−2.5	−1.6	−2.7	−1.7
Asp-18	<−2.4	−2.8	<−2.8	−2.8	<−3.4	−2.8	<−3.0	−2.7
Asp-74	−0.7	−0.7	−0.1	−0.2	−0.5	−0.7	−0.5	−0.5
Monomer b								
Lys-15	−2.5	−1.1	−2.4	−0.8	−2.7	−1.0	−2.7	−0.9
Tyr-78	−1.3	−0.8	−1.1	−0.8	−0.9	−0.8	−1.3	−0.9
Tyr-105	−0.1	−0.4	−0.6	−0.4	−0.4	−0.3	−0.7	−0.3
Tyr-116	−1.9	−1.0	−2.7	−0.7	−3.8	−1.0	−2.8	−1.0
His-56	−0.9	−0.9	−0.9	−0.7	−1.0	−0.7	−1.3	−0.8
His-88	<−1.6	−1.7	<−2.2	−1.7	<−1.8	−1.6	<−2.6	−1.7
His-90	−0.8	−0.4	−0.9	−0.5	−0.6	−0.5	−0.4	−0.3
Glu-51	−2.7	−0.8	−2.7	−0.9	−2.7	−0.6	−3.0	−0.8
Asp-18	<−2.8	−2.7	<−2.4	−2.6	−3.6	−2.6	<−2.4	−2.7

$\Delta pK_{1/2}$ values (($pK_{1/2}$(tetramer) – $pK_{1/2}$(dimer)) for the residues with the largest changes i.e., $|\Delta pK_{1/2}| > 0.6 \cong 0.8$ kcal/mol at 300 K. The values for the residues of only one dimer with the corresponding monomers a and b are shown. Due to symmetry we find similar behavior for the other dimer.

surements for different pH values. In a recent paper (Niraula et al., 2002) an energy difference of 4.3 kcal/mol between wild-type and the V30M mutant structure was reported at pH 7.1. This refers to absolute energy differences and not to relative ones as pH changes that we have analyzed in this work. Hydrogen exchange measurements (Liu et al., 2000) reveal an increase in structural fluctuations and local unfolding concomitant with the pH titration. As stressed above this is not currently directly predictable with the existing techniques. Nevertheless important residues that contribute to the pH instability are revealed. Moreover, as has been reported before (van Vlijmen et al., 1998a), the similarity of the results for all structures used, wild-type and mutant, supports the view that the mutations do not induce instability through a direct titration effect, but indirectly possibly by structural changes. Using dielectric constant 80 the free energy difference for dimer formation from the dimmers is 14.5, 14.4, 14.6, and 15.2 in kcal/mol for wt1, wt2, mut_noa, mut_a, and respectively and for the tetramer formation from the dimers is 5.6, 4.4, 6.5, and 6.2 kcal/mol for wt1, wt2, mut_noa, and mut_a, respectively, when we change the pH from 7 to 3.9. These values are comparable to the results we find using of dielectric 20. Using a dielectric constant of 80 the strength of the interactions between residues is reduced counterbalancing the absence of the solvation energy. We have also used GROMOS96 and PARSE force fields with no noticeable changes in the titration curves, and thus our calculations are robust with the change of the force field.

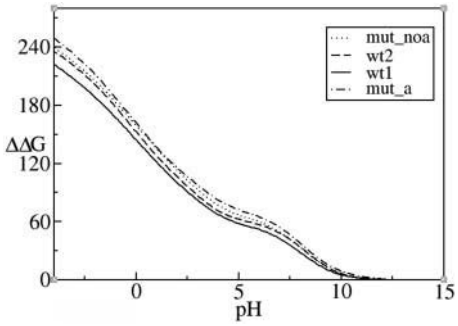

FIGURE 8 Free energy difference, $\Delta\Delta G$, in kcal/mol, upon tetramer formation from the monomers with $\varepsilon = 20$.

We thank the Wellcome Trust for a training fellowship in mathematical biology to S.S. and the Biotechnology and Biological Sciences Research Council for some of the computer resources. The work was carried out within the Bloomsbury Structural Biology Centre.

REFERENCES

Antosiewicz, J., J. A. McCammon, and M. K. Gilson. 1996. The determinants of pK_as in proteins. *Biochemistry*. 35:7819–7833.

Bashford, D., and K. Gerwert. 1992. Electrostatic calculations of the pKa values of ionizable groups in Bacteriorhodopsin. *J. Mol. Biol*. 224:473–486.

Bashford, D., and M. Karplus. 1990. pK_as of ionizable groups in proteins: atomic detail from a continuum electrostatics model. *Biochemistry*. 29:10219–10225.

Berendsen, H. J. C., D. van der Spoel, and R. van Drunen. 1995. GROMACS: A message-passing parallel molecular dynamics implementation. *Comput. Phys. Commun*. 91:43–56.

Beroza, P., D. R. Fredkin, M. Y. Okamura, and G. Feher. 1990. Protonation of interacting residues in a protein by a Monte-Carlo method: application to lysozyme and photosynthetic reaction center. *Proc. Natl. Acad. Sci. USA*. 88:5804–5808.

Blake, C. C. F., M. J. Geisow, S. J. Oatley, B. Rérat, and C. Rérat. 1978. Structure of prealbumin: secondary, tertiary and quaternary interactions determined by Fourier refinement at 1.8 Å. *J. Mol. Biol*. 121:339–356.

Damas, A. M., and M. S. Saraiva. 2000. Review: TTR amyloidosis-structural features leading to protein aggregation and their implications on therapeutic strategies. *J. Struct. Biol*. 130:290–299.

Demchuk, E., and R. C. Wade. 1996. Improving the continuum dielectrc approach to calculating pK_as of ionizable groups in proteins. *J. Phys. Chem*. 100:17373–17387.

Dobson, C. M. 1999. Protein misfolding, evolution, and disease. *Trends Biochem. Sci*. 24:329–332.

Gilson, M. K., and B. Honig. 1998. Calculation of the total electrostatic energy of macromolecular systems: solvation energies, binding energies, and conformational analysis. *Proteins*. 4:7–18.

Holst, M., and F. Saied. 1995. Numerical solution of the nonlinear Poisson-Boltzmann equation: developing more robust and efficient methods. *J. Compt. Chem*. 16:337–364.

Honig, B., and A. Nicholls. 1995. Classical electrostatics in biology and chemistry. *Science*. 268:1144–1149.

Hörnberg, A., T. Eneqvist, A. Olofsson, E. Lundgren, and A. E. Sauer-Eriksson. 2000. A comparative analysis of 23 structures of the amyloidogenic protein transthyretin. *J. Mol. Biol*. 302:649–669.

Kelly, J. W. 1997. Amyloid fibril formation and protein misassembly: a structural quest for insights into amyloid and prion diseases. *Structure*. 5:595–600.

Kelly, J. W. 1998. The alternative conformations of amyloidogenic proteins and their multi-step assembly pathways. *Curr. Opin. Struct. Biol.* 8:101–106.

Koradi, R., M. Billeter, and K. Wüthrich. 1996. MOLMOL: A program for display and analysis of macromolecular structures. *J. Mol. Graph.* 14:51–55.

Liu, K., H. S. Cho, H. A. Lashuel, J. Kelly, and D. E. Wemmer. 2000. A possible glimpse of a possible amyloidogenic intermediate of transthyretin. *Nat. Struct. Biol.* 7:754–757.

Nettleton, E. J., M. Sunde, Z. Lai, J. W. Kelly, C. M. Dobson, and C. V. Robinson. 1998. Protein subunit interactions and structural integrity of amyloidogenic transthyretins: evidence from electrospray mass spectrometry. *J. Mol. Biol.* 281:553–564.

Niraula, T. N., K. Haraoka, T. N. Niraula, K. Haraoka, Y. Ando, H. Li, H. Yamada, and K. Akasaka. 2002. Decreased thermodynamic stability as a crucial factor for familial amyloidotic polyneuropathy. *J. Mol. Biol.* 320:333–342.

Schaefer, M., M. Sommer, and M. Karplus. 1997. pH-Dependence of protein stability: absolute electrostatic free energy differences between conformations. *J. Phys. Chem B.* 101:1663–1683.

Simonson, T. 2001. Maclomolecular electrostatics: continuum models and their growing pains. *Curr. Opin. Struct. Biol.* 11:243–252.

Sitkoff, D., K. Sharp, and B. Honig. 1994. Accurate calculation of hydration free energies using macroscopic solvent models. *J. Phys. Chem.* 98:1978–1988.

Sheinerman, F. B., R. Norel, and B. Honig. 2000. Electrostatic aspects of protein-protein interactions. *Curr. Opin. Struct. Biol.* 10:153–159.

Ullmann, G. M., and E.-W. Knapp. 1999. Electrostatic models for computing protonation and redox equilibria in proteins. *Eur. Biophys. J.* 28:533–551.

van Gunsteren, W. F., S. R. Billeter, A. A. Eising, P. H. Hünenberger, P. Krüger, A. E. Mark, W. R. O. Scott, and I. G. Tironi. 1996. Biomolecular simulation: The GROMOS96 manual and user guide. Hochschulverlag AG an der ETH, Zurich.

van Vlijmen, H. W. T., S. Curry, M. Schaefer, and M. Karplus. 1998a. Titration calculations of Foot and Mouth Disease Virus Caspids and their Stabilities as a function of pH. *J. Mol. Biol.* 275:295–308.

van Vlijmen, H. W. T., M. Schaefer, and M. Karplus. 1998b. Improving the accuracy of protein pK_a calculations: Conformational averaging versus the average. *Proteins.* 33:145–158.

Warwicker, J., and H. C. Watson. 1982. Calculation of the electric potential in the active site cleft due to alpha-helix dipoles. *J. Mol. Biol.* 157:671–679.

Yang, A. S., and B. Honig. 1993. On the pH dependence of protein stability. *J. Mol. Biol.* 231:459–474.

Zauhar, R. Y., and A. Varnek. 1996. A fast and space-efficient boundary element method for computing electostatic and hydration effects in large molecules. *J. Comput. Chem.* 17:864–877.